A Bright Surprise: Live-Cell Labeling with Negatively Charged Fluorescent Probes based on Disulfonated Rhodamines and HaloTag

Dojin Kim+,[a] Stefan Stoldt+,[a, b, c] Michael Weber,[a] Stefan Jakobs,[a, b, c, d] Vladimir N. Belov,*[a] and Stefan W. Hell[a]

Disulfonated rhodamines are photostable and bright dyes widely used in life science and optical microscopy. However, disulfonated dyes were considered cell impermeable and not applicable in living cells. We challenged this assumption with 5 most popular rhodamines (Rho) having two carboxylic acid residues, versatile sulfonation patterns and emitting green (AS488), yellow (Rho530), orange (Rho565) and red (Rho590 and STAR RED) light. The probes comprising one rhodamine entity and a HaloTag™ amine (O2) ligand (x) were prepared and applied for labeling of living, *Vimentin-Halo* (*VIM-Halo*) expressing U-2 OS cells. Surprisingly, we observed specific and bright staining with simplest compounds Rho590-x, Rho565-x and Rho530-x bearing two negative charges; they performed well also in stimulated emission depletion (STED) microscopy. Specific staining and red shifts in absorption and emission bands were observed with other probes having one negative charge; they were prepared by native chemical ligation and esterification.

Introduction

The progress in the chemistry of functional dyes often sets pace in the advances of (bio)analytical chemistry, chemistry of materials and biology-related microscopy with optical super-resolution.[1] Rhodamines are favored by the users of fluorescent probes due to high brightness, photostability, diverse spectra and the availability of reactive dyes with various functional groups.[2] The natural drawbacks of non-polar fluorescent dyes are (self)aggregation (π-stacking) of planar fluorophores and non-specific labeling of cell organelles due to "sticking" of the emitters to lipophilic structures. To overcome these short-comings, polar groups are attached to the dye cores. In particular, the negatively charged groups are favored, as they improve imaging performance and reduce off-target binding more efficiently than the positively charged residues. Rhodamines, representing one of the most popular and well performing class of luminophores, are often decorated with two negatively charged sulfonic acid residues. The emission of sulfonated rhodamines and carborhodamines is particularly strong in aqueous solutions, insensitive to pH changes in a broad range, and these dyes found wide use in immunofluor-escence, including cell surface labeling.[3]

Importantly, specific labeling of living cells with disulfo-nated probes was not reported, because the general notion was that these dyes do not cross the outer and inner membranes of intact cells. On the other hand, many non-sulfonated fluores-cein derivatives,[4] rhodamines and carborhodamines,[5] as well as silicon-rhodamines,[6] have been applied as dye-linker-ligand assemblies for specific staining of living cells.[7] However, "live dyes" are limited to compact zwitterionic structures without charged groups. Most of the cell-permeate dyes are lipophilic, and their applicability in optical microscopy is often compro-mised by the drawbacks pertinent to the "naked" dye cores.

Surprisingly, the ligand-dependent labeling efficiency, spe-cificity and imaging performance of the fluorescent probes obtained from the common bis-sulfonated rhodamines re-mained unexplored.

We have chosen 5 disulfonated rhodamine dyes emitting light of various colors in the green to red spectral region (Scheme 1). As a reference dye we used rhodamine **Atto 532**. The sulfonic acid residues were attached to fluorophores in 3 different ways. The dyes were decorated with a HaloTag™ amine (O2) ligand[8] and applied for labeling the HaloTag – vimentin fusion in a stable cell line (live cells).[9] Fluorescence microscopy – confocal and STED – was used for evaluation of

[a] Dr. D. Kim,+ Dr. S. Stoldt,+ Dr. M. Weber, Prof. S. Jakobs, Dr. V. N. Belov, Prof. S. W. Hell
Department of NanoBiophotonics
Max Planck Institute for Multidisciplinary Sciences (MPI NAT)
Am Fassberg 11, 37077 Göttingen (Germany)
E-mail: vladimir.belov@mpinat.mpg.de

[b] Dr. S. Stoldt,+ Prof. S. Jakobs
Cluster of Excellence "Multiscale Bioimaging: from Molecular Machines to Networks of Excitable Cells" (MBExC)
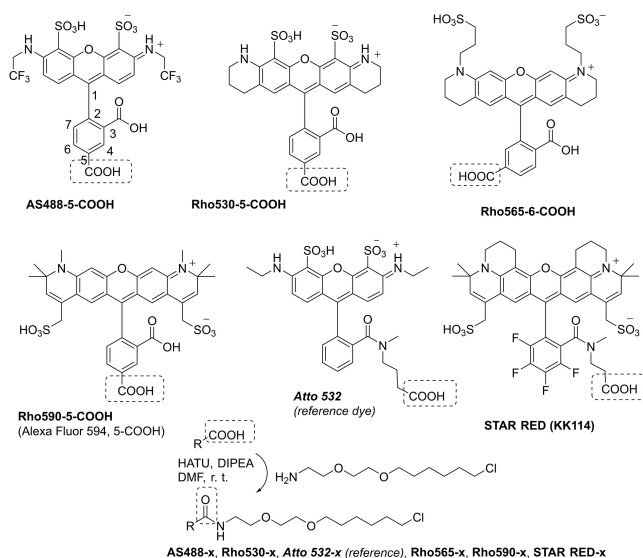University of Göttingen
37073 Göttingen (Germany)

[c] Dr. S. Stoldt,+ Prof. S. Jakobs
Clinic of Neurology
University Medical Center Göttingen
37099 Göttingen (Germany)

[d] Prof. S. Jakobs
Translational Neuroinflammation and Automated Microscopy
Fraunhofer Institute for Translational Medicine and Pharmacology
37075 Göttingen (Germany)

[+] These authors contributed equally to this work.

🖥 Supporting information for this article is available on the WWW under https://doi.org/10.1002/cmtd.202200076

Chemistry—Methods

Research Article
doi.org/10.1002/cmtd.202200076

Chemistry
Europe
European Chemical
Societies Publishing

Scheme 1. Sulfonated rhodamine dyes and amides prepared from HaloTag™ amine (O2). Atom numbering in the pendant phenyl ring with two carboxyl groups is uniform for all rhodamines and shown for **AS488-5-COOH**.

the labeling specificity and imaging performance of dye conjugates in live and fixed cells. Surprisingly, we observed specific and bright staining with **Rho590-x**, **Rho565-x** and **Rho530-x** bearing two negative charges (Scheme 1).

We tried further to improve imaging performance of disulfonated rhodamines prepared by selective amidation of the remote carboxyl group with the straight-chain HaloTag™ amine (Scheme 1). For branching the linker and varying the electrical charge of the probe, we used native chemical ligation (NCL, see Scheme 2),[10] thiol-maleimide addition and alkylation of the second, more sterically hindered carboxyl group attached to the dye core. Esterification of this carboxyl group provided a small red shift (+5…10 nm for absorption and emission

Scheme 2. Assembly of a dye – peptide – ligand conjugate: (a) native chemical ligation (NCL) followed by thiol-maleimide click reaction; (b) alkylation of a free carboxylic acid group with diazoalkane (e.g., diazomethane or diazoethane).
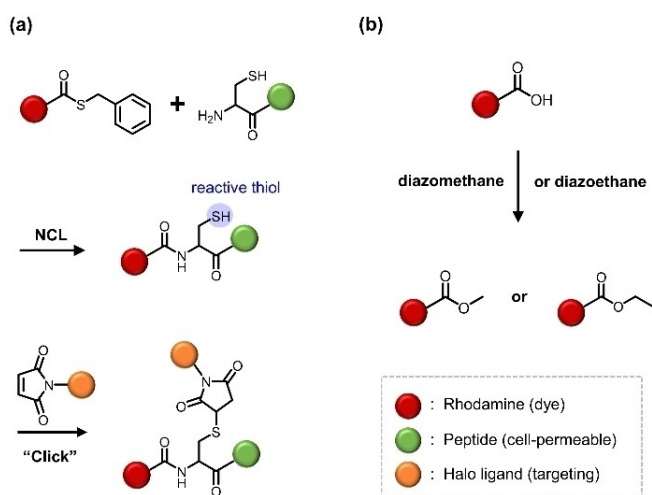
maxima) and removed one negative charge. Eventually, we prepared other probes, which provided specific staining and better interaction with the 775 nm STED laser. These were methyl or ethyl carboxylates **Rho590^Me-x**, **Rho565^Me-x**, **Rho530^Et-x** and the derivatives with a short dipeptide (all having one negative charge; see Figure 1).

Immunofluorescence labeling of two cellular proteins with **Rho565^Me-COOH** and the benchmark **STAR RED** dye (in fixed cells) provided minimal background and superior color separation compared to the reference pair (**Alexa Fluor 594** and **STAR RED**).

Results and Discussion

Molecular design and synthesis

We have chosen the dyes – **AS488-5-COOH**, **Rho530-5-COOH**, **Rho565-6-COOH**, **Rho590-5-COOH** and **STAR RED** (Scheme 1) – representing typical bis-sulfonated rhodamines and spanning the emission range from 520 to 660 nm (for spectral properties of all dyes, see Table 1). **AS488-5-COOH** (Abberior STAR 488) and **STAR RED** are commercially available from Abberior GmbH. **Rho530-5-COOH**[3a] and **Rho565-6-COOH**[11] were prepared according to the published procedures. **Rho590-5-COOH** is 5-carboxy isomer of the bright and photostable dye Alexa Fluor 594.[12] It was prepared by saponification of ethyl ester **Rho590-5-CO$_2$C$_2$H$_5$**[13] (for full description of the synthesis, see Scheme S2 and Supporting Information). **Alexa Fluor 594** is available from Thermo Fisher Scientific as 5- and 6-carboxy derivatives and conjugates with "small molecules". In aqueous buffers, "free" (unconjugated) dyes **Rho590-5-COOH**, **Rho565-6-COOH**, **Rho530-5-COOH** and **AS488-5-COOH** have a triple negative charge ($q=-3$): four anionic residues and the positively charged fluorophore. Due to the presence of three acidic centers and the positively charged fluorophore, **STAR RED** has a double negative charge in aqueous PBS buffer. In amides obtained upon conjugation of the dyes in Scheme 1 with HaloTag™ amine, the net electrical charges are −2 (**Rho590-x**, **Rho565-x**, **Rho530-x** and **AS488-x**), or −1 (**STAR RED-x**). The amides in Scheme 1 were prepared from free dyes and HaloTag® Amine (O2) in the presence of HATU and DIPEA. The yields varied from 48 to 95%, and the transformations were very fast (< 20 min at ambient temperature) and clean. These amides applied for labeling the HaloTag – vimentin fusion in a stable cell line (live cells).[9] Fluorescence microscopy – confocal and STED – was used for evaluation of the labeling specificity and imaging performance of dye conjugates in live and fixed cells. Surprisingly, we observed specific and bright staining already with simplest compounds **Rho590-x**, **Rho565-x** and **Rho530-x** bearing two negative charges (all applied as 2 μM and 500 nM solutions). They labeled the VIM-Halo fusions with quality comparable to the bench-mark probe **580CP-x** and performed well in stimulated emission depletion (STED) microscopy in living cells (Figures 2 and 3). The images of vimentin filaments observed with **AS488-x** were not as good as with other probes (see Figure S1). **STAR RED-x** provided some good

Chemistry—Methods

Research Article
doi.org/10.1002/cmtd.202200076

**Chemistry
Europe**
European Chemical
Societies Publishing

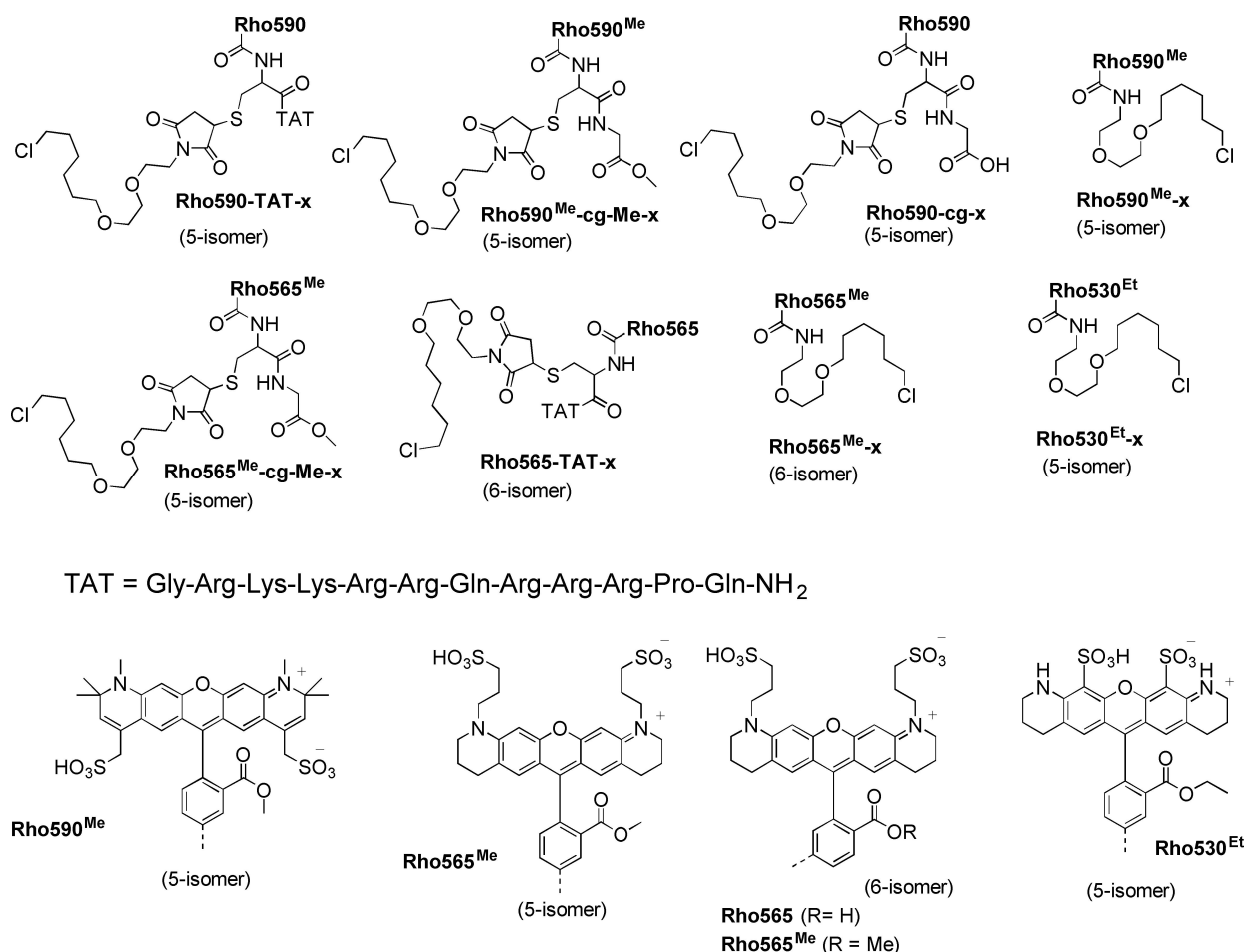TAT = Gly-Arg-Lys-Lys-Arg-Arg-Gln-Arg-Arg-Arg-Pro-Gln-NH$_2$

Figure 1. Fluorescent probes obtained according to Schemes 2, S1 and S2 2 from bis-sulfonated rhodamines **Rho590**, **Rho565**, **Rho530** and containing HaloTag^{TM} amine (O2) ligand H$_2$N(CH$_2$)$_2$O(CH$_2$)$_2$O(CH$_2$)$_6$Cl.

Table 1. Photophysical properties of free dyes STAR RED (KK114), Rho590-5-COOH (Alexa Fluor 594, 5′-COOH), Rho565-6-COOH, Rho530-5-COOH, AS488-5-COOH and their amides prepared from HaloTag^{TM} amine (O2) according to Scheme 1; measured in aqueous PBS buffer at pH 7.4.

	Absorption		Emission			Charge/imaging quality[c]
	λ_{max} [nm]	ε_{max} [M^{-1}cm^{-1}]	λ_{max} [nm]	Φ[a]	τ [ns][b]	
STAR RED (KK114)[d]	638	1.2×10^5	655	0.55	3.4	−2/
STAR RED-x	638	–	664	0.53	4.2	−1/−[e]
Rho590-5-COOH[f]	590	9.2×10^4	617	0.66	3.9	−3/
Rho590-x	588	–	621	0.72	4.1	−2/+++
Rho565-6-COOH	562	9.3×10^4	592	0.81	4.5	−3/
Rho565-x	565	–	592	0.73	4.7	−2/+++
Rho530-5-COOH[g]	531	7.4×10^4	555	0.99	4.1	−3/
Rho530-x	533	–	558	0.83	4.3	−2/++
Atto 532[h]	532	1.2×10^5	552	0.90	3.8	−2/
Atto 532-x	532	–	553	0.80	4.1	−1/±
AS488-5-COOH[i]	503	6.5×10^4	524	0.89	3.9	−3/
AS488-x	503	–	529	0.91	4.1	−2/±

[a] absolute values obtained with integrating sphere. [b] fitted to monoexponential model. [c] *580CP*-Halo[5c] was used as a reference probe; excellent (+ + +), very good (+ +), good (+), satisfactory (±), bad (−). [d] data of the manufacturer[17a]. [e] good results were observed in some experiments by using up to 6% v/v DMSO in the labeling medium. [f] data from ref. [12]. [g] data from ref. [3a]. [h] data of the manufacturer[17b]. [i] data of the manufacturer[17c].

images only in the presence of large concentrations of DMSO (up to 6%) in the labeling medium (see Figure S2); and even then the good results were not always reproducible.

Encouraged by these results, we tried to improve imaging performance of the probes having an amide group derived from the remote carboxyl function of rhodamine (Scheme 1).

Chemistry—Methods

Research Article
doi.org/10.1002/cmtd.202200076

Chemistry Europe
European Chemical
Societies Publishing

For branching the linker and varying the electrical charge of the probe, we used NCL reaction, thiol-maleimide addition and alkylation of the second, more sterically hindered carboxyl group attached to the dye core (Schemes 2, S1 and S2).

Thioesters required for NCL (Scheme 2a) were prepared from benzyl mercaptan and fluorescent dyes **Rho565-6-COOH** and **Rho590-5-COOH** (Scheme 1). The carboxylic acid groups at C-5 or C-6 in rhodamines are less sterically hindered than the carboxyl at C-3, and the reactions with thiols, amines, alcohols and other nucleophiles are selective. S-Benzyl thioesters **3**, **8**, and **9** (Scheme S1 and S2 in Supporting Information) were found to be stable by storage at $-20\,°C$ for at least 6 months (more stable than the corresponding S-phenyl thioesters). They readily participate in NCL, and therefore they were preferred as thioesters required for NCL (though S-phenyl thioesters are more reactive).

NCL was performed at room temperature in the buffer solution containing thiophenol (for details, see the Supporting Information). Thiophenol (in catalytic amounts) participates in an in situ *trans* thioesterification[14] and increased the reaction rate. TCEP was used as a strong reducing agent which blocked the formation of disulfide bonds. Under these conditions, thioester **3** readily bound with peptides having the N-terminal cysteine residue (Scheme 2a). We used the model dipeptide H-Cys-Gly-OH (yield 98%) or the so-called TAT peptide having the N-terminal cysteine residue (yield 69%; Figure 1 and Scheme S1).[15] The products of this step (Scheme 2a) have an amide bond at the ligation site (cysteine) with a free thiol residue. The thiol site is a strong nucleophile, which readily undergoes alkylation or participates in Michael addition involving the maleimide having the HaloTag® ligand attached to the nitrogen atom ("click" in Scheme 2a).

The new probes given in Figure 1 were prepared according to the general approach given in Scheme 2. The detailed reaction schemes with yields are given in Supporting Information (Scheme S1 and S2). By means of NCL, we prepared compounds **Rho590-cg-x**, **Rho590-TAT-x**, and **Rho565-TAT-x** incorporated the residues of the model cysteinylglucine dipeptide or cell-penetrating TAT peptide (with cysteine added to the N-terminus). **Rho590-TAT-x** (prepared from 5-carboxy isomer of the dye; Figure 1) was the first conjugate obtained with the inclusion of the TAT peptide residue.[15] It failed to specifically stain vimentin in living cells (Figure S3). Positional isomers might have different labeling specificities; therefore, another conjugate of the TAT peptide (**Rho565-TAT-x**) was synthesized from 6-carboxy isomer of the dye (Figure 1). We found that **Rho565-TAT-x** also did not provide specific staining of the Vimentin-HaloTag fusion protein. Therefore, we removed the TAT fragment and prepared the probes **Rho590-cg-x**, **Rho590Me-cg-Me-x** and **Rho565Me-cg-Me-x** which contain cysteinylglucine (Figure 1; see also Scheme S1 and S2). Each methylation (alkylation) of the carboxylic acid residue "removes" the negative charge and facilitates cell permeability of the product. Compounds with residues **Rho590Me**, **Rho565Me** and **Rho530Et** are methyl or ethyl carboxylates (Figure 1 and Scheme S2), in which the sterically shielded COOH groups (nearby the fluorophore) are esterified. For their syntheses, we used diazomethane or diazoethane as reagents. Methylation with diazomethane involves first the carboxylic acid groups (then, to some extent, the sulfonic acid residues). For example, compound **Rho590Me-cg-Me-x** with one negative charge has two methyl ester groups; it is polar and well-soluble in aqueous buffers due to the presence of the two sulfonic acid residues. Interestingly, a zwitterionic side product with zero net charge was detected by LC–MS, when one sulfonic acid residue was also methylated. The HPLC analysis of **Rho590Me-cg-Me-x** revealed 2 hardly resolved peaks (see Figure S4) with the same molecular mass (confirmed by LC–MS). They were assigned to two diastereomers, as the second asymmetric center is formed upon Michael addition (see Figure 1 and Scheme 2). We expected that **Rho590Me-cg-Me-x** ($q = -1$) would have a better cell-permeability than **Rho590-cg-x** ($q = -3$), will require low concentration of the probe in the staining solution and might provide better images than **Rho590-x**. Indeed, the probe **Rho590Me-cg-Me-x** (Figure 1) was found to provide specific staining in live cells (see the section below); therefore, we decided to prepare **Rho565Me-cg-Me-x** with another fluorophore, but otherwise the same structure.

The vast majority of commercial dyes (including **AS488** and **STAR RED**) are available as amino reactive *N*-hydroxysuccinimidyl (NHS) esters. We activated the dyes by transforming them into mono NHS esters (the remote, more sterically available COOH group reacts first; see Scheme S3) and isolated NHS esters in fairly good yields by means of preparative HPLC. Interestingly, the reaction of mono NHS esters with diazomethane involved the residual, more sterically shielded COOH group (see Scheme S3). The selected dyes were bound with secondary antibodies and applied in immunofluorescence staining of the fixed cells. The reactions of all NHS esters with secondary antibodies were carried out according to the standard procedure[16] (for details, see the Supporting Information). The degrees of labeling (DOL) for **Rho590Me-NHS** and **Rho565Me-NHS** dyes were calculated to be 4.2 and 3.1, respectively (for DOL measurements, see Supporting Information and Figure S5 and S6).

Photophysical properties

The dye **AS488-5-COOH** emits green light, it is the most short-wavelength emitter from the whole set. The direct sulfonation of the fluorophore and/or the presence of N-(2,2,2-trifluoroethyl) groups does not strongly influence the positions of absorption and emission bands, and the spectra of **AS488-5-COOH** remind these of Rhodamine 110. N-Alkylation (**Rho530**), N,N-dialkylation (**Rho565**), the presence of the two C=C bonds conjugated with fluorophore (**Rho590**, **STAR RED**), and four fluorine atoms (acceptor groups) in STAR RED shift the absorption and emission bands more and more to the red spectral region. **Rho530-COOH** emits orange light, while **Rho565-COOH** and **Rho 590-COOH** emit brick red and cherry red light, respectively (for a photo, see Figure S7). Table 1 contains data for free dyes and their amides prepared from HaloTag™ amine (O2) according to Scheme 1. The photo-

physical properties of more complex dye derivatives (Figure 1) are given in Table 2. The photophysical properties were measured in aqueous PBS buffer at pH 7.4 (see Figures S8–S10 and Tables 1 and 2). All dyes have high fluorescence quantum yields (> 0.5 in aqueous solutions), large ε-values ($0.65-1.2 \times 10^5 \text{ M}^{-1} \text{ cm}^{-1}$) and fluorescence lifetimes (3.4–4.7 ns) typical for rhodamines.

We studied and compared the influence of the dye core and the substituents (a peptide linker; COOH or COOAlk group at C-3) on the positions of the absorption and emission bands. Alkylation of the sterically hindered carboxylic acid group at C-3 results in small red shifts of absorption and emission maxima (2–7 nm and 10–12 nm, respectively). The influence of the long TAT peptide is weak (red shift of 4–5 nm for both absorption and emission). All dyes feature very similar band shapes and relatively small Stokes shifts (ca. 30 nm). Methylation of COOH group at C-3 slightly decreases the fluorescence lifetime, and the addition of the TAT-peptide slightly increases the fluorescence lifetime. Overall, the good photophysical properties of the initial dyes and their amides (Table 1) were maintained upon NCL and/or methylation reactions, with only slight changes (compare the data in Tables 1 and 2).

The absorption and emission spectra of esters **Rho590**[Me]**-x**, **Rho565**[Me]**-x**, **Rho530**[Et]**-x** and **STAR RED-x**, with imaging results in confocal and STED microscopy discussed in the next section, are given in Figure 2. The absorption and emission maxima are in the range from 530 nm to 590 nm and from 560 nm to 630 nm, respectively. Esterification of the sterically shielded COOH group at C-3 in the phenyl ring provides small red shift in the spectra, increases absorption at 775 nm (STED laser) and improves STED performance of the probes origination from **Rho565**[Me] and **Rho590**[Me] fluorophores. The absorption of **Rho530**[Et] dye core at 775 nm is very low, and the STED effect at this wavelength is negligible.

Table 2. Photophysical properties of more complex dye derivatives from Figure 1; measured in aqueous PBS buffer at pH 7.4.

	Absorption λ_{max} [nm]	Emission λ_{max} [nm]	Φ[a]	τ [ns][b]	Charge/imaging quality[c]
Rho590-cg-x[d]	588	623	0.66	4.2	−3/+
Rho590[Me]-cg-Me-x[d]	595	633	0.60	3.9	−1/±
Rho590-TAT-x[d]	592	627	0.62	4.4	+6/−
Rho590[Me]-x[d]	593	629	0.65	3.9	−1/+ +
Rho565[Me]-cg-Me-x[d]	569	604	0.68	4.5	−1/±
Rho565-TAT-x[e]	570	596	0.63	5.0	+6/−
Rho565[Me]-x[e]	567	602	0.70	4.3	−1/+ +
Rho530[Et]-x[e]	537	537	0.79	4.2	−1/+

[a] absolute values obtained with integrating sphere. [b] fitted to monoexponential model. [c] *580CP*-Halo[5c] was used as a reference probe; excellent (+ + +), very good (+ +), good (+), satisfactory (±), bad (−). [d] obtained from 5-COOH isomer of the dye. [e] obtained from 6-COOH isomer of the dye.
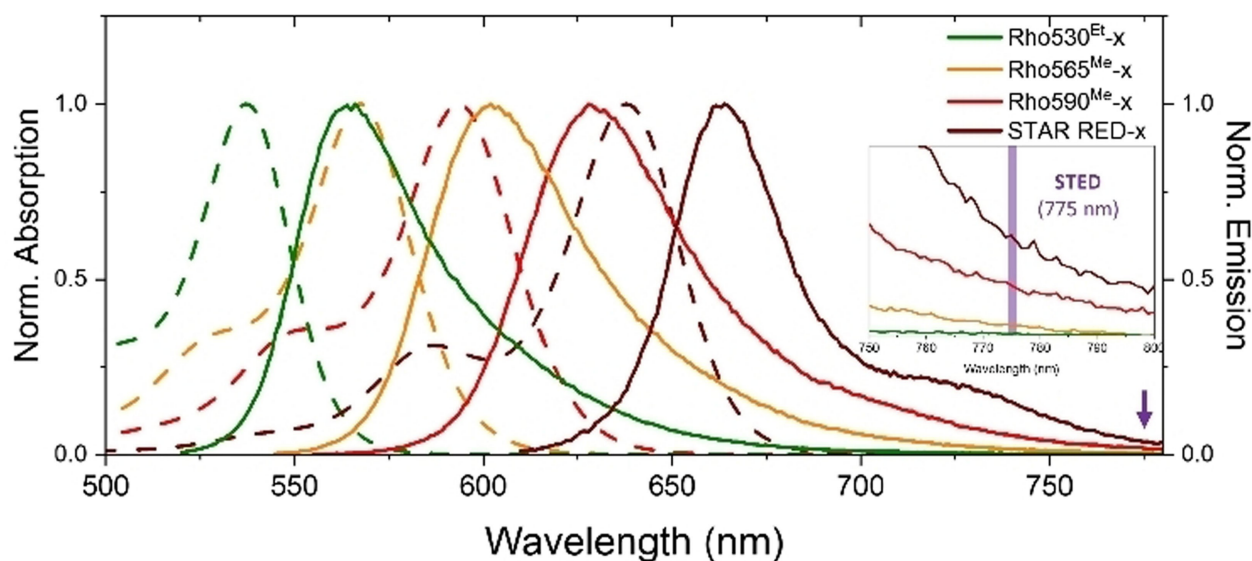

Figure 2. Normalized absorption (dashed lines) and emission spectra (solid lines) of STAR RED-x (brown), **Rho590**[Me]**-x** (red), **Rho565**[Me]**-x** (orange), and **Rho530**[Et]**-x** (green); $c = 10$ μM in aqueous PBS buffer, pH 7.4. The insert shows relative emission intensities at the STED wavelength (775 nm).

Chemistry—Methods

Research Article
doi.org/10.1002/cmtd.202200076

Chemistry
Europe
European Chemical
Societies Publishing

Confocal and super-resolution STED imaging in living and fixed cells

The newly synthesized amides having the residue of the HaloTag[TM] ligand were characterized in terms of labeling and imaging performance in living cells, and suitability for light microscopy. For that, we used living, monoclonal, *VIM-Halo* expressing Human Osteosarcoma (U-2 OS) cells.[9] Genetically unmodified U-2 OS cells were used in immunofluorescence experiments (labeling in fixed cells). As reference probes, we used **Atto532-x**[18] (Scheme 1) and **580CP-x**[5c] with 1,8-disulfonated rhodamine (q = −1) and carbopyronine (q = 0, zwitterionic and compact) fluorophores, respectively. For comparison, all probes were applied at concentrations of 2 μM and 500 nM, with a labeling time of 60 min (for details, see the Supporting Information; in particular, Figure S11). **Atto532-x** provided satisfactory images, and 580-CP – very good ones (Figure 3). Expectedly, the STED effect with 775 nm STED laser was not observed with an **Atto532-x** probe.

Most surprisingly, the simplest conjugates of unmodified dyes with the HaloTag (O2) amine – **Rho590-x**, **Rho565-x**, **Rho530-x** and **AS488-x** – provided the best images, in spite of the fact that their net electrical charge was −2 and the cell-permeability was expected to be low. Obviously, the non-polar and lipophilic HaloTag[TM] amine (O2) improved the labeling efficiency of the fluorescent probes. Probably, a $(CH_2)_6$ chain and the chlorine atom facilitated the cell permeability; while the negative charge of the probe prevented the unspecific binding with intracellular structures and facilitated the transport of the unbound probe out of the cell interior. To compare the labeling results, we stained live cells at two concentrations of the probes "Dye-x" in the working solutions −2 μM and 0.5 μM. As shown in Figure S11, the confocal images were comparably good for all probes and at both concentrations. In particular, the staining efficiency of 5-carboxy isomer of **Rho565-x** was very similar to that of 6-carboxy isomer. These positional isomers have the same photophysical and labeling properties.

Next, we tested a series of conjugates (Tables 1, 2 and Figure 3) with COOR (R=H, Me, Et) group at C-3 and, in some cases, an additional dipeptide (CG) attached to the second carboxylic acid group (at C-5 or C-6). The net electrical charge varied from −3 (**Rho590-cg-x**) to −1 (Table 1). All probes shown in Figure 3 provided satisfactory to excellent labeling: specific, with minimal background, comparable in quality with the benchmark probe **580CP-x** and superior to **Atto532-x**. **STAR RED-x** (KK114-x in Figure 3) worked well only for freshly prepared dye samples and in the presence of 6% (v/v) DMSO in the labeling solution; even then it was difficult to acquire the high-quality pictures in all experiments.

As mentioned above, **Rho590-TAT-x** and **Rho565-TAT-x** (q = +6) proved unsuitable for specific labeling of VIM-Halo fusion protein (see Figure S3). Nevertheless, these compounds were cell permeable and showed unspecific staining of the whole cells, even leading to an enrichment within the nucleoli of the cell nucleus.

For all compounds shown in Figure 3, a STED laser with an emission wavelength of 775 nm was used. As expected, the STED performance decreased in the row **STAR RED** – **Rho590** – **Rho565** – **Rho530** due to decrease in the dye emission intensity at 775 nm (see Table S1). The low emission cross-section at 775 nm decreases the depletion effect for the probes based on **Rho565** fluorophore and makes the resolution improvement practically unobservable for **Rho530** and **Atto532** dyes. In fact, **Rho530** and **Atto532** dyes were designed for the use with the STED laser emitting at 660 nm (LEICA Microsystems).

The probe **AS488-x** provided satisfactory labeling and observable resolution improvement, when excitation at 485 nm and a STED laser emitting at 595 nm were applied (see Figure S1). The live cell STED imaging in this spectral area is challenging, due to phototoxic effects of the excitation and STED beams "amplified" by the presence of a rhodamine dye generating reactive oxygen species (ROS), and also due to the relatively high natural emission of the cellular structures in the blue-green spectral region.

For the investigation of cellular processes, it is important to assess the sub-cellular distribution and colocalization of proteins with the highest possible optical resolution. This can be achieved by dual color STED nanoscopy via labeling of two different proteins with specific serums in fixed cells followed by detecting the primary antibodies with a dye conjugated secondary antibodies. The use of 775 nm STED laser results in superior STED performance, compared to other STED wavelengths of 660 nm or 595 nm. For 775 nm dual color STED, the dye pair **STAR RED** (exc. max = 640 nm) and **Alexa Fluor 594** (exc. max = 594 nm) became a standard dye pair, resulting in images with superior resolution, high signal to noise ratio and a relatively low amount of crosstalk.[19] Nevertheless, and especially for STED setups with fixed detection filter sets (Figure S12), the strong emission of **Alexa Fluor 594** often results in undesirable signal in the channel intended for **STAR RED** detection. Based on these features, we studied the use of **Rho565[Me]-COOH** coupled to secondary antibodies as an alternative to **Alexa Fluor 594**. The **Rho565[Me]** fluorophore has a blue-shifted excitation spectrum (compared with **Alexa Fluor 594**) that better fits the detection window 580 nm–630 nm. For testing and comparing the dyes, we labeled the fixed U-2 OS cells with a Tom22 specific serum and detected the primary antibody via secondary ones coupled either to **Alexa Fluor 594**, or **Rho590[Me]**, or **Rho565[Me]**. We compared the immunofluorescence stainings for their bleaching behavior under confocal (Figure S13) and STED imaging conditions (Figure S14), and also for the amount of observable cross-talk (Figure S15). We found that in confocal imaging (Figure S13) and under STED conditions (Figure S14), **Rho590[Me]** was more photostable than **Alexa Fluor 594** and showed the lowest bleaching rate of these three dyes. In the first frames, the emission of **Rho590[Me]** even increased. This effect is often observed for the lipophilic dyes, like **Atto 647N**, **STAR 580**, etc.[20] Probably, it is due to dissociation of the aggregated dye residues caused by irradiation. Next we compared the relative cross-talk of the three dyes by plotting the signal distribution between the "red" detection window (650–720 nm) and both detection windows: 580–630 nm and 650–720 nm (Figure S14). We found the lowest

Chemistry—Methods

Research Article
doi.org/10.1002/cmtd.202200076

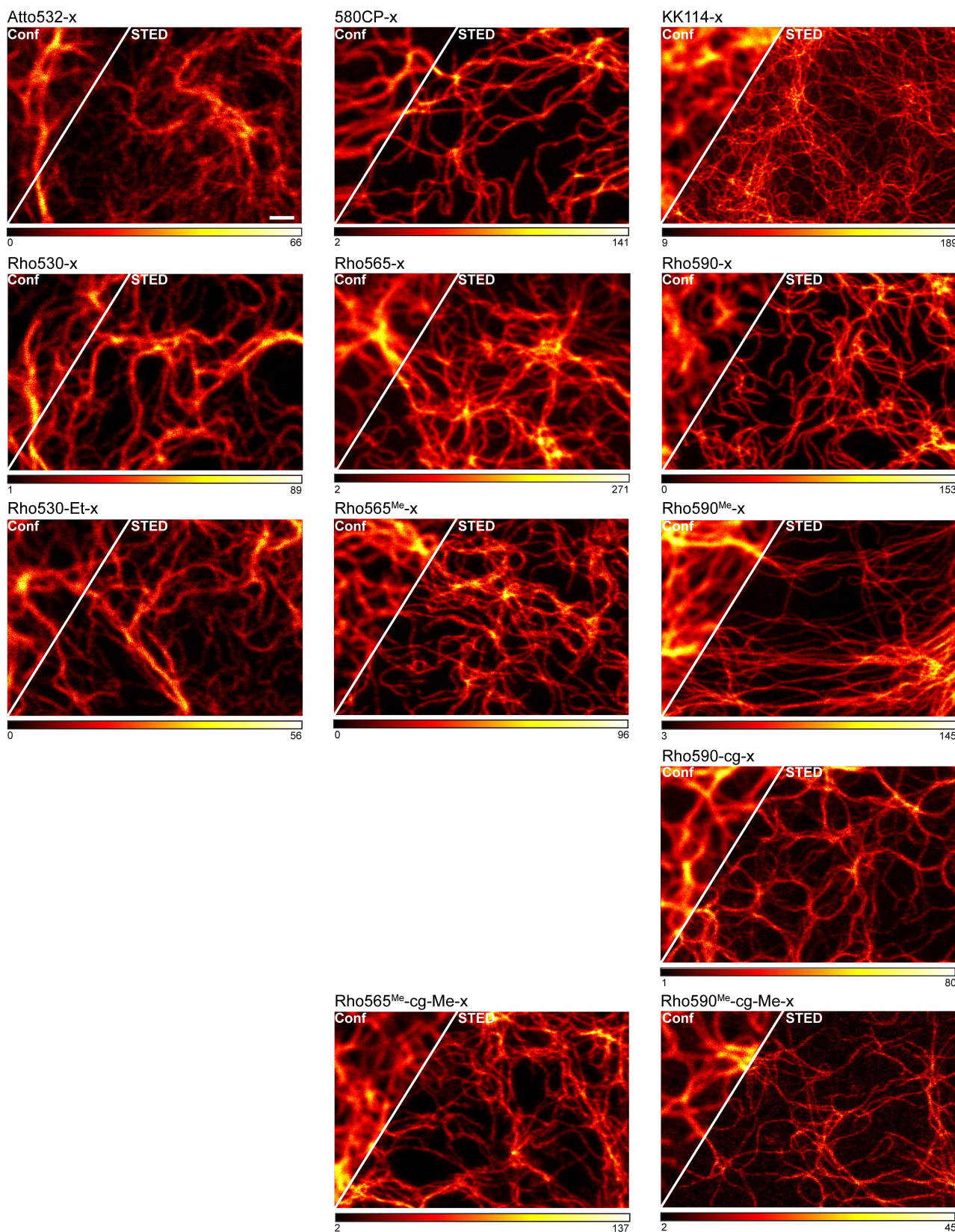**Chemistry Europe**
European Chemical
Societies Publishing

Figure 3. Rhodamine Halo Ligands are suitable for live cell STED nanoscopy. Confocal and STED images of U-2 OS cells expressing *Vimentin-Halo* from the endogenous locus. Cells were labeled with 2 μM of the Halo Tag Ligands (x) of Atto532, *580CP* (reference dyes with 1,8-disulfonated rhodamine and non-sulfonated carbopyronine fluorophores, respectively), KK114 (STAR RED), **Rho530, Rho565, Rho590, Rho530^{Et}, Rho565^{Me}, Rho590^{Me}, Rho590-cg, Rho565^{Me}-cg-Me** and **Rho590^{Me}-cg-Me**. For structures, see Figure 1 and Scheme 1. Images of the probes originating from the same fluorophores (except reference dyes in the 1st row) are arranged in columns, and similar chemical modifications are arranged in rows. Scale bar: 1 μm.
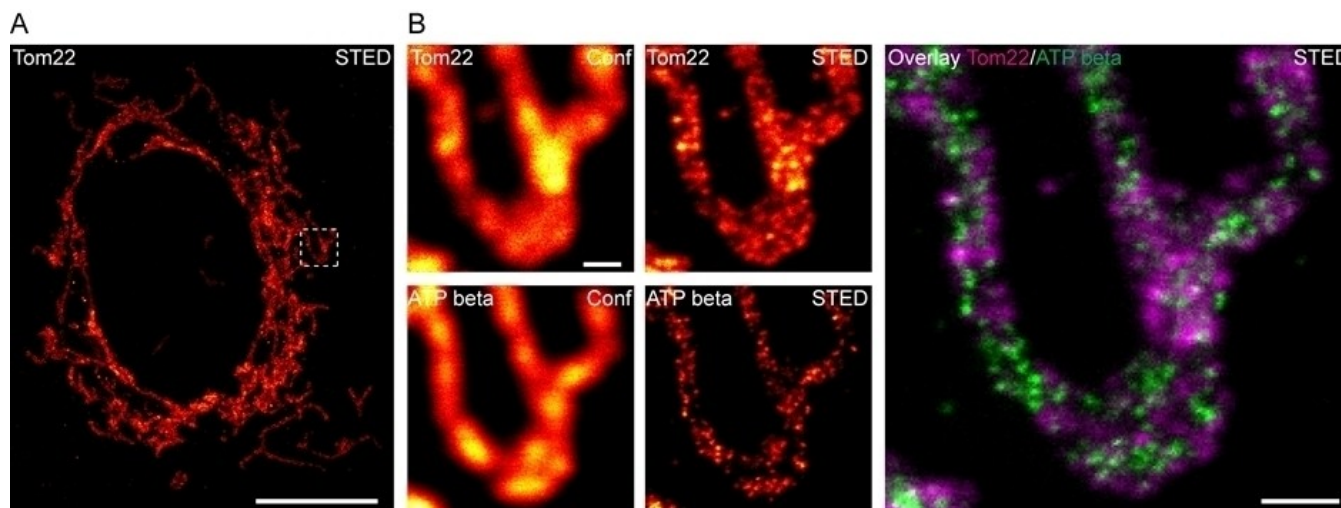
Figure 4. Antibody staining on fixed cells: Rho565[Me] in two color STED imaging. (A, B) STED nanoscopy images of fixed U-2 OS cells decorated with antibodies specific for Tom22 and ATP beta respectively. Secondary antibodies to detect the Tom22 antibody were coupled to **Rho565[Me]** (Figure 1), the secondary antibodies to detect ATP beta were coupled to **STAR RED** (Scheme 1) respectively. (B) Confocal and STED magnifications and the overlay of the STED channels of the area indicated in (A). Scale bars: 10 μm (A), 500 nm (B).

cross-talk for **Rho565[Me]** fluorophore, closely followed by **Alexa Fluor 594** (Rho590).

Finally, we tested the dye pair **Rho565[Me]** and **STAR RED** in two-color imaging experiments (Figure 4 and Figure S12). For that, we used formaldehyde fixed U-2 OS cells and labeled them with antibodies specific for two mitochondrial proteins. One of them was Tom22 – a subunit of the translocase of the mitochondrial outer membrane. Another one was the protein ATP beta, a subunit of the mitochondrial ATP synthase, a protein complex localized in the mitochondrial inner membrane. The secondary antibodies to detect the Tom22 antibody were coupled to **Rho565[Me]-COOH**, and the secondary antibodies to detect ATP beta were coupled to Abberior **STAR RED**. The STED images shown in Figure 4 demonstrate the applicability and good performance of the dye pair **Rho565[Me]** and **STAR RED** in the dual color STED nanoscopy. The clear separation of protein clusters and negligible cross-talk between the detection channels were observed. Taken together, the fluorophore **Rho565[Me]** showed better bleaching behavior and significantly lower cross-talk than **Alexa Fluor 594**. At the same time, the STED performance **Rho565[Me]** was comparable to **Alexa Fluor 594**. We envisage, however, a slightly lower optical resolution and brightness of **Rho565[Me]**, at least on the commercially available setup used in this study. The dual color STED microscopy with antibodies relates to fixed cells, but since it helped to choose a pair of dyes providing good color separation, one of them (applied as **Rho590[Me]-x**, Table 2) may be combined with the cell permeant probes of various colors and used in living cells.

Conclusion

The dyes bearing two negative charges were considered inapplicable for selective and vital labeling. Surprisingly, we observed specific and bright staining of the living cells already with the simplest fluorescent probes comprised of disulfonated rhodamine dyes and the HaloTag[TM] amine (O2) ligand (**Rho590-x, Rho565-x,** and **Rho530-x**). These probes labeled the VIM-Halo fusions as good as the reference conjugate **580CP-x**,[5c,f] and performed equally well or even better in stimulated emission depletion (STED) microscopy. It will be interesting to apply the SNAP-tag fusions[21] or other protein tags and try to find the probes providing specific staining with the negatively (or positively, like the famous Atto 647 N dye[22]) charged fluorescent probes. Still, the negatively charged dyes are widespread and have many advantages: high solubility in aqueous buffers, stable emission over a wide range of pH, low aggregation and negligible background fluorescence. Like the HaloTag, the SNAP-tag provides covalent binding with a target, but the labeling of the SNAP-tag fusions proceeds slower than the labeling of the HaloTag fusion proteins, and the task may be more challenging. However, due to the high solubility and low unspecific binding of the negatively charged probes, it may be possible to apply higher concentrations of the working solutions and achieve specificity also with the negatively charged fluorescent probes recognizing the SNAP-tag fusions.

Conflict of Interest

The authors declare no conflict of interest.

Data Availability Statement

The data that support the findings of this study are available in the supplementary material of this article.

[1] a) M. Fernandez-Suarez, A. Y. Ting, *Nat. Rev. Mol. Cell Biol.* **2008**, *9*, 929–943; b) A. G. Godin, B. Lounis, L. Cognet, *Biophys. J.* **2014**, *107*, 1777–1784; c) J. B. Grimm, B. P. English, J. Chen, J. P. Slaughter, Z. Zhang, A. Revyakin, R. Patel, J. J. Macklin, D. Normanno, R. H. Singer, T. Lionnet, L. D. Lavis, *Nat. Methods* **2015**, *12*, 244–250; d) S. J. Sahl, S. W. Hell, S. Jakobs, *Nat. Rev. Mol. Cell Biol.* **2017**, *18*, 685–701.

[2] a) M. Beija, C. A. Afonso, J. M. Martinho, *Chem. Soc. Rev.* **2009**, *38*, 2410–2433; b) S. N. Uno, M. Kamiya, T. Yoshihara, K. Sugawara, K. Okabe, M. C. Tarhan, H. Fujita, T. Funatsu, Y. Okada, S. Tobita, Y. Urano, *Nat. Chem.* **2014**, *6*, 681–689.

[3] a) V. P. Boyarskiy, V. N. Belov, R. Medda, B. Hein, M. Bossi, S. W. Hell, *Chem. Eur. J.* **2008**, *14*, 1784–1792; b) N. Panchuk-Voloshina, R. P. Haugland, J. Bishop-Stewart, M. K. Bhalgat, P. J. Millard, F. Mao, W.-Y. Leung, R. P. Haugland, *J. Histochem. Cytochem.* **1999**, *47*, 1179–1188; c) M. Trumpp, A. Oliveras, H. Gonschior, J. Ast, D. J. Hodson, P. Knaus, M. Lehmann, M. Birol, J. Broichhagen, *Chem. Commun.* **2022**, *58*, 13724–13727.

[4] a) J. B. Grimm, T. A. Brown, A. N. Tkachuk, L. D. Lavis, *ACS Cent. Sci.* **2017**, *3*, 975–985; b) K. Hirabayashi, K. Hanaoka, T. Takayanagi, Y. Toki, T. Egawa, M. Kamiya, T. Komatsu, T. Ueno, T. Terai, K. Yoshida, M. Uchiyama, T. Nagano, Y. Urano, *Anal. Chem.* **2015**, *87*, 9061–9069.

[5] a) F. Bottanelli, E. B. Kromann, E. S. Allgeyer, R. S. Erdmann, S. Wood Baguley, G. Sirinakis, A. Schepartz, D. Baddeley, D. K. Toomre, J. E. Rothman, J. Bewersdorf, *Nat. Commun.* **2016**, *7*, 10778; b) J. Bucevičius, J. Keller-Findeisen, T. Gilat, S. W. Hell, G. Lukinavičius, *Chem. Sci.* **2019**, *10*, 1962–1970; c) A. N. Butkevich, G. Y. Mitronova, S. C. Sidenstein, J. L. Klocke, D. Kamin, D. N. H. Meineke, E. D'Este, P.-T. Kraemer, J. G. Danzl, V. N. Belov, S. W. Hell, *Angew. Chem. Int. Ed.* **2016**, *55*, 3290–3294; *Angew. Chem.* **2016**, *128*, 3350–3355; d) R. Gerasimaitė, J. Seikowski, J. Schimpfhauser, G. Kostiuk, T. Gilat, E. D'Este, S. Schnorrenberg, G. Lukinavičius, *Org. Biomol. Chem.* **2020**, *18*, 2929–2937; e) F. Grimm, S. Nizamov, V. N. Belov, *ChemBioChem* **2019**, *20*, 2248–2254; f) G. Lukinavičius, G. Y. Mitronova, S. Schnorrenberg, A. N. Butkevich, H. Barthel, V. N. Belov, S. W. Hell, *Chem. Sci.* **2018**, *9*, 3324–3334.

[6] a) M. Fu, Y. Xiao, X. Qian, D. Zhao, Y. Xu, *Chem. Commun.* **2008**, 1780–1782; b) E. Kim, K. S. Yang, R. J. Giedt, R. Weissleder, *Chem. Commun.* **2014**, *50*, 4504–4507; c) Y. Koide, Y. Urano, K. Hanaoka, T. Terai, T. Nagano, *ACS Chem. Biol.* **2011**, *6*, 600–608; d) Y. Koide, Y. Urano, K. Hanaoka, W. Piao, M. Kusakabe, N. Saito, T. Terai, T. Okabe, T. Nagano, *J. Am. Chem. Soc.* **2012**, *134*, 5029–5031; e) G. Lukinavičius, L. Reymond, E. D'Este, A. Masharina, F. Göttfert, H. Ta, A. Güther, M. Fournier, S. Rizzo, H. Waldmann, C. Blaukopf, C. Sommer, D. W. Gerlich, H.-D. Arndt, S. W. Hell, K. Johnsson, *Nat. Methods* **2014**, *11*, 731–733; f) G. Lukinavičius, L.

Reymond, K. Umezawa, O. Sallin, E. D'Este, F. Göttfert, H. Ta, S. W. Hell, Y. Urano, K. Johnsson, *J. Am. Chem. Soc.* **2016**, *138*, 9365–9368; g) G. Lukinavičius, K. Umezawa, N. Olivier, A. Honigmann, G. Yang, T. Plass, V. Mueller, L. Reymond, I. R. Corrêa Jr, Z.-G. Luo, C. Schultz, E. A. Lemke, P. Heppenstall, C. Eggeling, S. Manley, K. Johnsson, *Nat. Chem.* **2013**, *5*, 132–139; h) T. E. McCann, N. Kosaka, Y. Koide, M. Mitsunaga, P. L. Choyke, T. Nagano, Y. Urano, H. Kobayashi, *Bioconjugate Chem.* **2011**, *22*, 2531–2538; i) T. Pastierik, P. Šebej, J. Medalová, P. Štacko, P. Klán, *J. Org. Chem.* **2014**, *79*, 3374–3382; j) P. Shieh, M. S. Siegrist, A. J. Cullen, C. R. Bertozzi, *Proc. Natl. Acad. Sci. USA* **2014**, *111*, 5456–5461; k) B. Wang, X. Chai, W. Zhu, T. Wang, Q. Wu, *Chem. Commun.* **2014**, *50*, 14374–14377; l) T. Wang, Q.-J. Zhao, H.-G. Hu, S.-C. Yu, X. Liu, L. Liu, Q.-Y. Wu, *Chem. Commun.* **2012**, *48*, 8781–8783; m) A. N. Butkevich, M. L. Bossi, G. Lukinavičius, S. W. Hell, *J. Am. Chem. Soc.* **2019**, *141*, 981–989.

[7] a) A. N. Butkevich, V. N. Belov, K. Kolmakov, V. V. Sokolov, H. Shojaei, S. C. Sidenstein, D. Kamin, J. Matthias, R. Vlijm, J. Engelhardt, S. W. Hell, *Chem. Eur. J.* **2017**, *23*, 12114–12119; b) J. B. Grimm, A. N. Tkachuk, L. Xie, H. Choi, B. Mohar, N. Falco, K. Schaefer, R. Patel, Q. Zheng, Z. Liu, J. Lippincott-Schwartz, T. A. Brown, L. D. Lavis, *Nat. Methods* **2020**, *17*, 815–821.

[8] G. V. Los, L. P. Encell, M. G. McDougall, D. D. Hartzell, N. Karassina, C. Zimprich, M. G. Wood, R. Learish, R. F. Ohana, M. Urh, D. Simpson, J. Mendez, K. Zimmerman, P. Otto, G. Vidugiris, J. Zhu, A. Darzins, D. H. Klaubert, R. F. Bulleit, K. V. Wood, *ACS Chem. Biol.* **2008**, *3*, 373–382.

[9] A. N. Butkevich, H. Ta, M. Ratz, S. Stoldt, V. N. Belov, S. W. Hell, *ACS Chem. Biol.* **2018**, *13(2)*, 475–480.

[10] P. Dawson, T. Muir, I. Clark-Lewis, S. Kent, *Science* **1994**, *266*, 776–779.

[11] C. Barnes, N. N. Romanov, WO/2007/135368, **2007**.

[12] For the photophysical properties of Alexa 594: I. Johnson, M. Spence, "The Molecular Probes Handbook: A Guide to Fluorescent Probes and Labeling Technologies" can be found under http://www.thermofisher.com/handbook, **2010**.

[13] K. Kolmakov, C. A. Wurm, D. N. Meineke, F. Gottfert, V. P. Boyarskiy, V. N. Belov, S. W. Hell, *Chem. Eur. J.* **2014**, *20*, 146–157.

[14] P. E. Dawson, M. J. Churchill, M. R. Ghadiri, S. B. H. Kent, *J. Am. Chem. Soc.* **1997**, *119*, 4325–4329.

[15] A. D. Frankel, C. O. Pabo, *Cell* **1988**, *55*, 1189–1193.

[16] M. Weber, M. Leutenegger, S. Stoldt, S. Jakobs, T. S. Mihaila, A. N. Butkevich, S. W. Hell, *Nat. Photonics* **2021**, *15*, 361–366.

[17] a) https://abberior.shop/abberior-STAR-RED; b) http://www.atto-tec.com/ATTO-532.html?language=en; c) https://abberior.shop/abberior-STAR-488.

[18] For the structure and the spectra of the free dye, see: http://www.atto-tec.com/ATTO-532.html.

[19] a) L. Große, C. A. Wurm, C. Brüser, D. Neumann, D. C. Jans, S. Jakobs, *EMBO J.* **2016**, *35*, 402–413; b) S. Stoldt, T. Stephan, D. C. Jans, C. Brüser, F. Lange, J. Keller-Findeisen, D. Riedel, S. W. Hell, S. Jakobs, *Proc. Natl. Acad. Sci. USA* **2019**, *116*, 9853–9858; c) T. Stephan, C. Brüser, M. Deckers, A. M. Steyer, F. Balzarotti, M. Barbot, T. S. Behr, G. Heim, W. Hübner, P. Ilgen, F. Lange, D. Pacheu-Grau, J. K. Pape, S. Stoldt, T. Huser, S. W. Hell, W. Möbius, P. Rehling, D. Riedel, S. Jakobs, *EMBO J.* **2020**, *39*, e104105.

[20] G. Y. Mitronova, S. Polyakova, C. A. Wurm, K. Kolmakov, T. Wolfram, D. N. H. Meineke, V. N. Belov, M. John, S. W. Hell, *Eur. J. Org. Chem.* **2015**, 337–349.

[21] A. Keppler, S. Gendreizig, T. Gronemeyer, H. Pick, H. Vogel, K. Johnsson, *Nat. Biotechnol.* **2003**, *21*, 86–89.

[22] a) Y. Han, Z. Zhang, W. Liu, Y. Yao, Y. Chen, X. Luo, W. Wang, Y. Xu, X. Liu, C. Kuang, X. Hao, *BioRxiv preprint* **2020**, https://doi.org/10.1101/2020.05.10.086538; b) Y. Han, Z. Zhang, W. Liu, Y. Yao, Y. Xu, X. Liu, C. Kuang, X. Hao, *Frontiers in Chem.* **2021**, *8*, article 601436.

RESEARCH ARTICLE

Dr. D. Kim, Dr. S. Stoldt, Dr. M. Weber, Prof. S. Jakobs, Dr. V. N. Belov*, Prof. S. W. Hell

1 – 10

A Bright Surprise: Live-Cell Labeling with Negatively Charged Fluorescent Probes based on Disulfonated Rhodamines and HaloTag
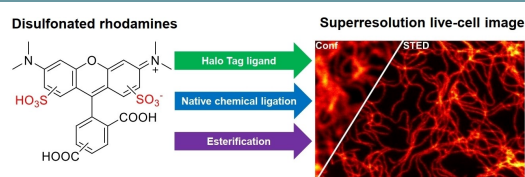
Disulfonated rhodamines were considered cell impermeable and not applicable for specific labeling in live cells. Surprisingly, in spite of the double negative charge of the molecules, the conjugates of these popular dyes with the HaloTag™ amine (O2) ligand showed specific and bright live staining (demonstrated by confocal and super-resolution microscopy).